

Article

Distribution and Transport of Thermal Energy within Magma–Hydrothermal Systems

John Eichelberger 

International Arctic Research Center, University of Alaska Fairbanks, Fairbanks, AK 99775, USA;
jceichelberger@alaska.edu

Received: 15 April 2020; Accepted: 25 May 2020; Published: 1 June 2020



Abstract: Proximity to magma bodies is generally acknowledged as providing the energy source for hot hydrothermal reservoirs. Hence, it is appropriate to think of a “magma–hydrothermal system” as an entity, rather than as separate systems. Repeated coring of Kilauea Iki lava lake on Kilauea Volcano, Hawaii, has provided evidence of an impermeable, conductive layer, or magma–hydrothermal boundary (MHB), between a hydrothermal system and molten rock. Crystallization on the lower face of the MHB and cracking by cooling on the upper face drive the zone downward while maintaining constant thickness, a Stefan problem of moving thermal boundaries with a phase change. Use of the observed thermal gradient in MHB of 84 °C/m yields a heat flux of 130 W/m². Equating this with the heat flux produced by crystallization and cooling of molten lava successfully predicts the growth rate of lava lake crust of 2 m/a, which is faster than simple conduction where crust thickens at \sqrt{t} and heat flux declines with $1/\sqrt{t}$. However, a lava lake is not a magma chamber. Compared to erupted and degassed lava, magma at depth contains a significant amount of dissolved water that influences the magma’s thermal, chemical, and mechanical behaviors. Also, a lava lake is rootless; it has no source of heat and mass, whereas there are probably few shallow, active magma bodies that are isolated from deeper sources. Drilling at Krafla Caldera, Iceland, showed the existence of a near-liquidus rhyolite magma body at 2.1 km depth capped by an MHB with a heat flux of ≥ 16 W/m². This would predict a crystallization rate of 0.6 m/a, yet no evidence of crystallization and the development of a mush zone at the base of MHB is observed. Instead, the lower face of MHB is undergoing partial melting. The explanation would appear to lie in vigorous convection of the hot rhyolite magma, delivering both heat and H₂O but not crystals to its ceiling. This challenges existing concepts of magma chambers and has important implications for use of magma as the ultimate geothermal power source. It also illuminates the possibility of directly monitoring magma beneath active volcanoes for eruption forecasting.

Keywords: magma energy; magma convection; hydrothermal system; heat flux; geothermal energy; eruption

1. Introduction

Given the tremendous difference between the rate of heat transport by conduction through solid rock and advection of heat by aqueous fluid through permeable rock, the strong control of hydrothermal activity on magma evolution cannot be questioned. It is therefore surprising that relatively little has been written on this topic. The reason is likely a separation of communities of practice. Until now, no one has investigated magmatic systems directly. Rather, experiments are conducted with micro synthetic or natural rock samples in the laboratory, field and petrologic studies explore “fossil” systems, remote (surface or supra-surface-based) sensing detects proxy signals of magma from active systems, and hydrodynamic models describe how magma could behave, subject to various assumptions. In contrast, hydrothermal systems are the domain of fluid geochemistry and alteration mineralogy,

reservoir modeling involving porous flow, and most importantly, direct measurement of conditions and lithology from geothermal drilling, much of the data from which are proprietary.

There are notable exceptions to the inadequate treatment of the magma–hydrothermal coupling problem. For example, Lister [1] provided rigorous theoretical treatment of thermal cracking and crystallization, defining a moving magma–hydrothermal boundary (MHB), a Stefan problem, related to mid-ocean ridge volcanism. Hardee [2] applied this approach to analyzing temperature measurements from Kilauea Iki lava lake. Carrigan [3] drew an analogy between magma–hydrothermal systems and two resistors in series, where the largest resistance, the hydrothermal system, dominates energy flow. He previously argued for convection in magma bodies and large sills [4,5], which would keep the value of the magma resistor low, whereas convection in lava lakes would die out quickly. This is in contrast to, for example, Hort et al. [6], who asserted that a mush insulator grows at the top of the magma body and quickly shuts off convection. Recently, Lamy et al. [7] continued the view of simple inward-growing mush and stagnant magma, although their main point was the importance of a magmatic vapor phase (MVP) released during crystallization of intrusions. Hawkesworth et al. [8] made assumptions about heat loss from magma bodies through hydrothermal systems and concluded that the more vigorous hydrothermal circulation expected at shallow depth would force more rapid magmatic differentiation. Fournier [9] used advective heat discharge by rivers draining the Yellowstone Plateau to infer crystallization rates of the underlying magma. Scott et al. [10] modeled high-enthalpy fluid circulation above a heat source at magmatic temperature. Glazner [11], making arguments similar to those employed here, showed the importance of hydrothermal convection above magma and then further argued that an arid climate favors the development of large magma chambers.

The purpose of this paper is to discuss new implications beginning to emerge from accidental encounters with magma by geothermal drilling and the importance of understanding MHB. It is in part a review paper, gathering key observations where hidden bodies of magma have been accidentally encountered. Complementing these are lessons learned from drilling into a lava lake as a magma chamber analogue. Possible explanations for the more surprising drilling results are proposed. The drilling data are sparse, however, so it is not possible to consider all allowable interpretations or to say that the postulates are uniquely constrained by the data. Rather, the intent is to stimulate thinking about the magma–hydrothermal connection, leading to direct observations through intentional scientific drilling into this critical zone [12]. In contrast, a lava lake is an imperfect analogue. It represents magma that has erupted and degassed to become lava, losing almost all of its dissolved water, which profoundly affects melt properties and phase relationships. A lava lake is also rootless, closed to introduction of heat and mass from below, whereas probably few shallow magma chambers exist in isolation from complex melt-bearing columns that extend from the mantle [13]. The only way to truly understand magma with its surrounding crust is to drill it.

2. Drilling into Molten Rock

It may come as a surprise that molten rock can be drilled [14]. Normal drilling practice is to circulate fluid down the drill stem, through the drill bit, and back up the annulus to the surface. The cold fluid is mostly water, usually with some additives. It serves the purposes of keeping the drill bit and the rock cool and returning rock, brittlely fractured in making the hole, to the surface. These fragments are in the form of sand-like cuttings. However, if a core bit and receiving core barrel are used, samples are retrieved as cylinders of rock. The core is of greater use scientifically because the exact depth of origin is known and the samples are intact, preserving a great deal of information about lithologic texture, interrelationships, structures such as veins, and temperature and chemical gradients.

Molten rock can be drilled if circulation is sufficiently fast and penetration sufficiently slow to quench melt to brittle drillable glass just ahead of the advancing drill bit. Magma, unerupted molten rock stored at depth, has never been cored, but in principle it could be. The molten rock in the interior of lava lakes has been cored many times for research purposes, most prominently in Hawaii where

the occurrence of pit (collapse) craters frequently results in ponding of lava of sufficient depth to remain molten for years or decades. This reveals much about how magma crystallizes.

The most thoroughly studied lava lake is Kilauea Iki (Figure 1 [15]). Erupted near the summit of Kilauea Volcano in 1959 and filled to a depth of 130 m, it was cored many times during the next three decades. Thus, a thorough record of its cooling and crystallization was accumulated [16]. I am aware of three sites, the Puna site on Kilauea Volcano, Hawaii [17]; Menengai Caldera in the East African Rift, Kenya [18,19]; and Krafla Caldera, Iceland [20], where drilling has penetrated silicic magma. There may well be other incidents that have not been reported in the publicly accessible literature, or cases where return of glass cuttings was not recognized as evidence of magma. The most comprehensively studied case of actual magma is the Iceland Deep Drilling Program's IDDP-1 [21], drilled to a depth of 2104 m in Krafla Caldera, Iceland in 2009. The richness of the data is because IDDP-1 was a research and development well sponsored by a consortium of Icelandic geothermal companies, with extensive scientific participation under the aegis of the International Continental Scientific Drilling Program (ICDP). However, the objective of the well was to penetrate the domain of supercritical fluids at 4.5 km, where both temperature and fluid pressure were expected to be above the critical point of water. Instead, magma was encountered at 2.1 km, with a temperature well above the critical point but fluid pressure below it. IDDP-1 can now be viewed as opening the path to extensive exploration of the magma body it discovered, the objective of the Krafla Magma Testbed program (KMT [12]).

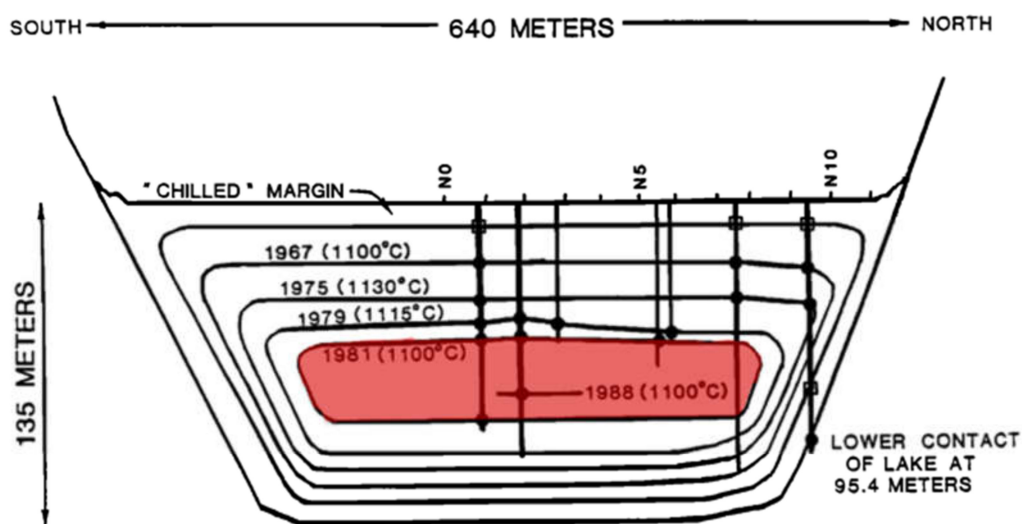


Figure 1. Cross section of Kilauea Iki lava lake showing some of the holes that have been cored and the position of the molten lava lens with time. 1981 (Figure 2A) is shown in red [15].

Table 1 is a compilation of pertinent data and calculation results for magma–hydrothermal systems. It makes sense that the first encounters with magma were shallow ones. However, are these oddities or are there many more such bodies to be encountered as drilling in quest of high-enthalpy fluids proceeds to greater depth? Superhot wells are expensive from a geothermal perspective, some USD \$20 M for IDDP-1. One would infer that the reason why there is little scientific data from magma and near-magma encounters, other than from IDDP-1, is the economic pressure to make a well “pay” as soon as a viable hydrothermal resource is reached. It will take an alliance of scientists, engineers, and geothermal companies as pioneered by IDDP to really explore and put to use this final crustal frontier.

One striking feature of the compilation in Table 1, in addition to magma being unexpected, is that it is surprisingly shallow. Another is the absence of an upper crystallization or mush zone above the nearly pure melt magma. One could say that the magma intruded only just before drilling or that

the upper mush zone, which would be gravitationally unstable, had only just collapsed. However, this is special pleading, and a general explanation would be that this is the way magma chambers work.

I will summarize the most pertinent lessons from Kilauea Iki, and then apply them, to the extent they can be, to the much sparser data set from Krafla and other systems. As a note on terminology, I use magma to refer to a material comprising silicate melt +/-crystals +/-vapor bubbles that is capable of flow, usually considered to require melt ≥ 50 vol%. [22]. At < 50 vol%, I use mush to denote residual melt-bearing material that is the product of partial crystallization of magma, and partially melted rock (in the Krafla case felsite) to denote rock that is undergoing melting. Distinguishing between residual melt in mush and partial melt in melting rock is based on texture. Residual melt in mush is interstitial to generally euhedral crystals. Partial melt in partially melted rock is interstitial to crystals that are anhedral and contain embayments, indicative of resorption. In the former, crystals were growing from melt when quenched, in the latter they were dissolving into melt.

Table 1. Some modeling and drilling results pertaining to magma–hydrothermal systems.

Site	Lister Model	Kilauea Iki, Hawaii	Heimaey, Iceland	Grimsvotn Caldera, Iceland	Puna Venture, Hawaii	Menengai Caldera, Kenya	Krafla Caldera, Iceland
Setting	theory	Basalt lava lake	Basalt lava flow	Central volcano in plate rift	Magma in east Kilauea rift	Caldera in East African Rift	Central volcano in plate rift
Depth to magma/lava (m)	Diking at midocean ridge	0 @ 1959, 80@1988	—	>2000	2488	2080	2102
Roof rock	—	Own crust	Own crust	basalt	Diorite w/melt inclus.	syenite	Partially melted felsite
wt% SiO ₂	Generic basalt	50 bulk, 75 last melt	48–50	51 basalt	67 dacite	63 trachyte	75 rhyolite
T (°C) where melt present	—	1000–1190	1030–1055	1100	1050	—	900
vol% Xtal	—	variable	—	—	5–8	<5	<1
Viscosity (Pa·s)	—	variable	—	10–2000	10 ⁷	—	3 × 10 ⁵
Flow up well (m)	—	0 in 1981	—	—	14	0	9
Last erupted silicic magma	—	—	—	—	never	8000 a	10 ⁴ a; (trace in 1724)
ΔT/ΔZ (°C/m) in MHB	—	84	10,000	300	>5	>17	>16
MHB thickness (m)	—	11	0.1	2	—	—	<25
Heat flux W/m ²	—	130	40,000	120–600	—	—	>24
Thermal power output (MW)	—	14	300 (short term)	1000–5000	—	—	>100 from IDDP-1
Fracture penetration rate	30 m/a	2 m/a	1 m/day	5 m/a	—	—	—
Permeability therm. cracks	10 D	0.3	—	—	—	—	0.7
References	[1]	[2,15,16]	[23]	[23–25]	[17]	[18,19]	[20,26,27]

3. The Case of Kilauea Iki: A Stefan Problem

The results from drilling Kilauea Iki have been influential in thinking about magma chambers at depth, particularly results pertaining to the transition from the hydrothermal zone of the solid lake crust to the melt-rich zone [2]. The hydrothermal zone comprises basalt with fractures open to the surface and contains steam from vaporization of downward percolating rainwater. At the surface elevation of the lake of 1070 m, the boiling point is 96 °C, and the temperature profile is isothermal at that temperature to the base of the open system. The downward transition from the brittle, fractured, crystalline hydrothermal regime to the molten regime is a thin conductive, linear temperature gradient zone that has moved downward with time. The hydrothermal zone expanded downward by cooling the crust and cracking it towards the retreating melt zone (Figure 2). The result is that cooling and crystallization are approximately constant so that crustal thickness grows linearly with time (Figure 2C) conductive zone, essentially a growing layer of insulation. However, thermally, the transition zone, MHB, can be treated as bounded by two constant temperature surfaces bathed by hydrothermal fluid on the upper surface and melt-rich lava on the lower surface, producing a steady-state condition within the moving spatial coordinates of the zone [2]. The downward propagation of MHB is then a proxy for the thermal power output of the system.

Bjornsson et al. [23] suggested that the phenomena described above accounted for the high, constant thermal energy output of Grimsvotn Volcano, Iceland. They also noted the formation of columnar jointing (Figure 2B) within the lava flow at Heimaey, Iceland, where water from firehoses was used to stop a lava flow threatening to block the harbor. Fournier [9] likewise appealed to invasion of thermal cracking to enhance latent and sensible heat extraction from the very large magma body inferred to exist at Yellowstone, producing an advective thermal power output of 5 GW. Axelsson et al. [29] made a similar suggestion for IDDP-1 at Krafla, where an extended flow test yielded a thermal power output exceeding 100 MW. Thermal cracking was investigated experimentally by Lamur et al. [30], who found that it can begin during cooling as early as 100 °C below the solidus.

Kilauea Iki is the only case where the MHB concept can be quantitatively tested through a time series of temperature profiles and thicknesses of the crust. The temperature gradient in the conductive zone (using thermal parameters of Hardee [2] so as to be consistent) gives the heat flow in the z direction (F_z):

$$F_z = -k \Delta T / \Delta z \quad (1)$$

where thermal conductivity, k , is 1.57 J/m·s·°C and the average, linear (conductive) thermal gradient, $\Delta T / \Delta z$, is between the solidus at 1000 °C and the hydrothermal system at 100 °C using data from years 1962, 1967, 1979, and 1981 (data: [16]) is 84 °C/m. Therefore:

$$F_z = -130 \text{ W/m}^2$$

The total thermal power output (P_T) is the product of heat flux and area, A :

$$P_T = F_z A \quad (2)$$

Using melt lens radius $r = 186 \text{ m}$ from Figure 1, A is $1.6 \times 10^5 \text{ m}^2$ and:

$$P_T = 14 \text{ MW}$$

The rate of growth of the volume of the crust of the lake is a proxy for power output. This is to say that the product of the rate of downward propagation of the solidus ($\Delta z_{1000} / \Delta t$) times the energy density of molten lava cooled to the solidus (ϵ_M), should equal the heat flux upward measured by the temperature gradient in the conductive zone (Figure 2A). To test this, we can solve for the predicted rate of thickening of the crust with heat flux, F_z , calculated with Equation (1).

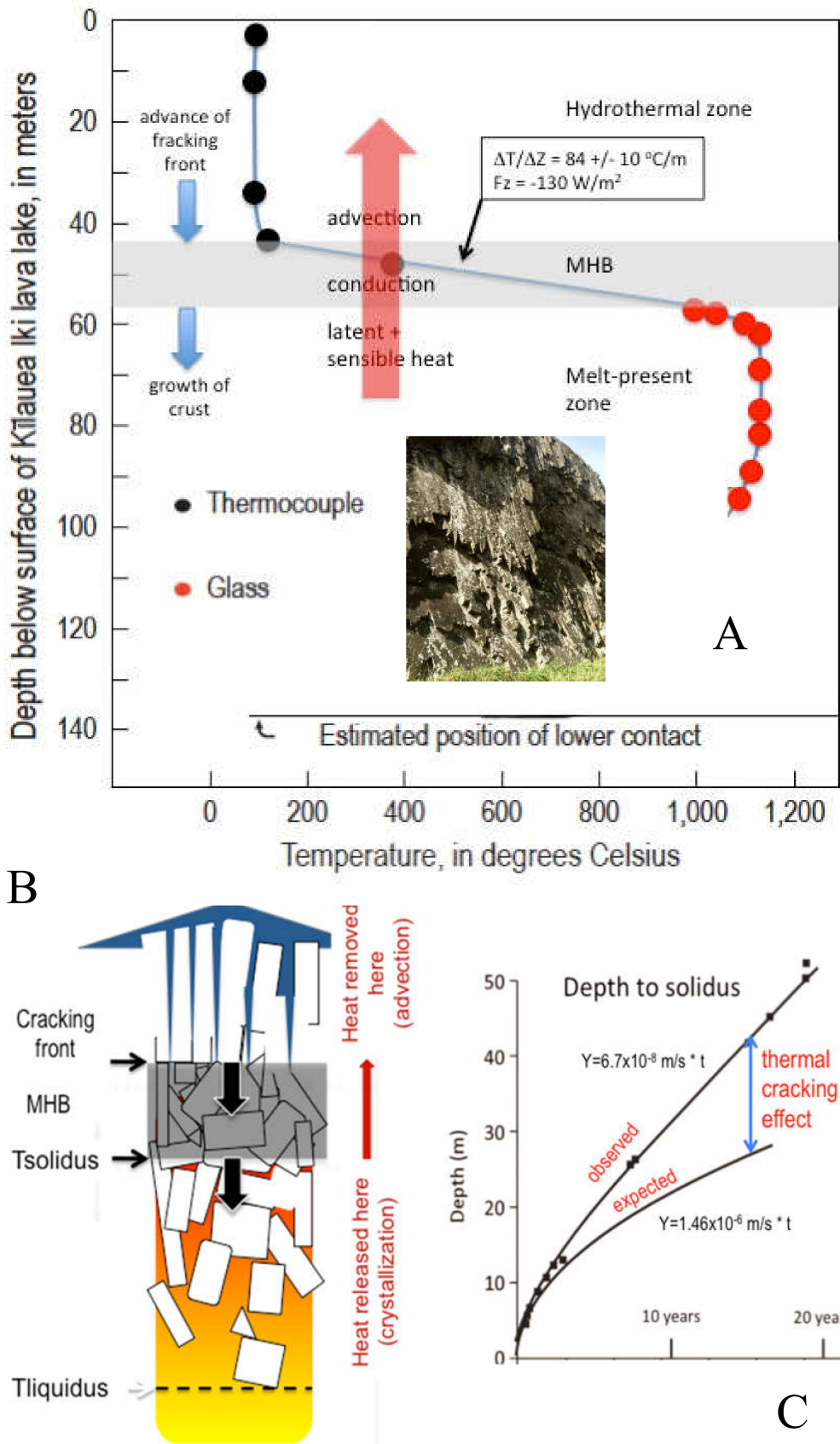


Figure 2. (A) A temperature profile from the surface into the melt lens in Kilauea Iki, 1981 (after

Helz [16]). This is one of many obtained over three decades after formation of the lake in 1959. A conductive MHB, moving downward by thermal cracking, divides a hydrothermal zone at local boiling temperature from the molten zone. Inset shows thermal contraction columns in a lava flow near Christ Church, NZ, the track left by a descending MHB (photo by author). (B) Cartoon displaying the processes envisioned for a cooling igneous body, based upon observations at Kilauea Iki. The tips of the contraction fractures define a thermal cracking front that propagates perpendicular to and following the retreating isotherms. The fractures define the familiar columnar jointing. (C) Core hole data on growth of crust over two decades show the effect of thermal cracking compared to that of simple conduction with crystallization (after Hardee [2] using the Carslaw and Jaeger thermal model [28]).

One can define an effective heat capacity of basalt lava, β_{Meff} , within the interval T_L to T_S :

$$\beta_{Meff} = \beta_M + \frac{L_M}{T_L - T_S} \quad (3)$$

where $\beta_M = 1046 \text{ J/kg}\cdot^\circ\text{C}$, sensible heat capacity of molten basalt lava

$L_M = 418,000 \text{ J/kg}$, latent heat of crystallization of molten basalt lava

$T_L = 1150 \text{ }^\circ\text{C}$, liquidus temperature and

$T_S = 1000 \text{ }^\circ\text{C}$, solidus temperature

$\Delta Z_{1000}/\Delta t$, downward velocity of solidus

$\rho_M = 2700 \text{ kg/m}^3$, mass density of molten basalt

$\rho_B = 2900 \text{ kg/m}^3$, mass density of basalt

Using the above values in Equation (3) gives:

$$\beta_{Meff} = 3800 \text{ J/kg}\cdot^\circ\text{C}$$

Energy density of magma, ε_M , i.e., energy per volume released by cooling from T_L to T_S , is:

$$\varepsilon_M = \rho_M \beta_{Meff} (T_L - T_S) \quad (4)$$

Yielding by volume (adjusted from molten density) of crystallized basalt:

$$\varepsilon_B = 1.7 \times 10^9 \text{ J/m}^3$$

For the rate of movement of T_S downward ($\Delta z_{1000}/\Delta t$; growth of crust) to produce the heat flux upward:

$$\varepsilon_B (\Delta Z_{1000}/\Delta t) = Fz \quad (5)$$

Solving for the downward growth rate of the crust:

$$\Delta Z_{1000}/\Delta t = 7.6 \times 10^{-8} \text{ m/s or } 2.4 \text{ m/a}$$

The observed value for 1962 to 1981 is $7.4 \times 10^{-8} \text{ m/s}$ or 2.3 m/a . This agreement is somewhat fortuitous because it is better than the uncertainties should provide and neglects that some latent heat of crystallization has already been lost. Nevertheless, if the lava lake is a good analogue for a magma chamber, then the conductive temperature gradient in the MHB can be used to determine the heat flux from magma to the hydrothermal system and to predict the rate of growth of a crystal layer at the roof of the magma chamber.

4. The Case of Krafla

Figure 3 is a plausible 3-D rendering of Krafla, centered at 65.71° N and 16.75° W . The encounter with magma by drilling was not anticipated through geophysical surveys. However, it was later shown

that the Krafla rhyolite magma body coincided with a strong V_p/V_s anomaly [31] and its top with a seismic reflector [32].

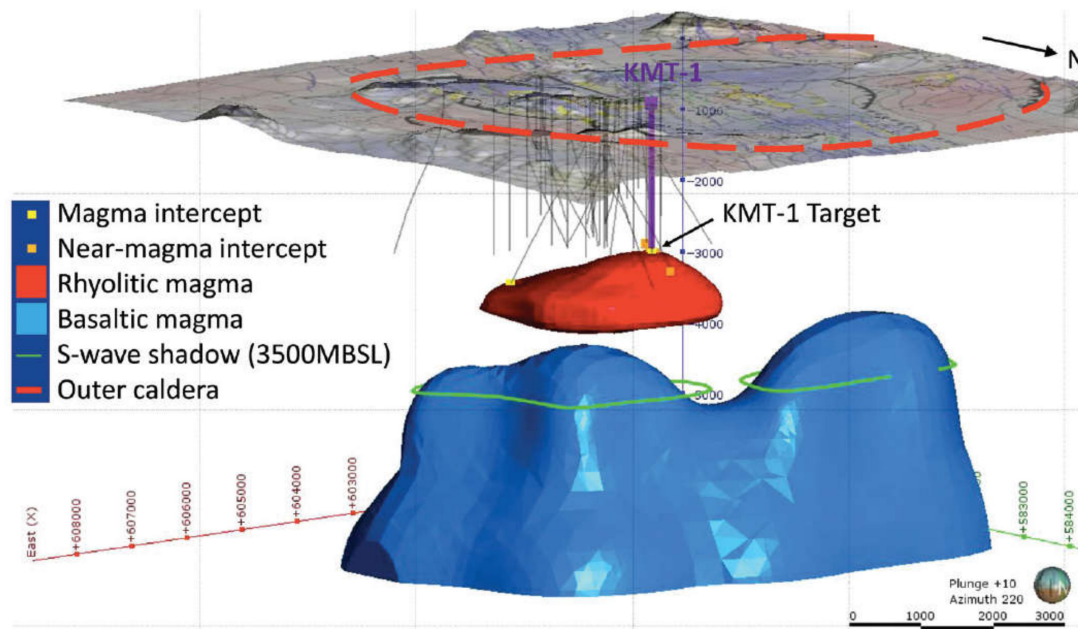


Figure 3. Idealized configuration of rhyolitic magma body (red) and deeper basaltic body (blue) under Krafla Caldera (red dashed line). Light gray lines are existing wells drilled by Landsvirkjun (National Power Company). The heavy line is planned KMT-1, the first well of KMT [12], closely following the path of IDDP-1 [21]. Credit: J.W. Catley. In addition to IDDP-1, two other wells have penetrated or come close to rhyolite magma. There is much debate about the configuration of the rhyolitic magma, ranging from small separate pockets or a larger, long-persistent unified body similar to what erupted from Askja in 1875 [33]. There is more general acceptance of the large persistent basaltic body shown in blue, which receives new basaltic injections, sends out N–S dikes during rifting “Fires”, and is responsible for the two S-wave shadow zones and for most of the surface deformation.

The site for IDDP-1 was chosen to be near the center and hottest part of the caldera. It is also close to Viti Crater, site of a phreatomagmatic explosion during the Myvatn Fires in 1724 that ejected a small amount of rhyolite similar to magma of IDDP-1. As the most prominent example of drilling encountering rhyolite magma, results were presented in a special issue of Geothermics (2014) and in a number of separate publications; note especially [26,27,34].

In drilling IDDP-1, circulation was lost at 2070 m, and continued drilling encountered a soft formation at an average depth of 2102 m in the original well and two sidetracks. It is the second sidetrack (third penetration) that is of special interest here because magma flowed up the borehole, the bit became stuck, and for a brief period, restoration of circulation brought glass-bearing chips (Figure 4) to the surface, confirming that magma was present at the bottom of the well (Figure 5). Gamma logs indicate that lithology below 2070 m is predominantly felsite (A in Figure 5, fine-grained crystalline equivalent of rhyolite magma) through this zone [26]. The deepest temperature measurements are at 2077 m and through multiple measurements are extrapolated to an equilibrium formation temperature of 500 °C (Figures 5 and 6) [26]. Somewhere between that depth and the melt-present zone (B in Figure 5, checkered) should be a transition from brittle to ductile behavior in the felsite. This should be the lower limit of fracturing. However, high strain rates caused by cooling during drilling would have raised the temperature of the brittle/ductile boundary so that fractures could have propagated deeper. Only two kinds of melt-present (shown by quenched glass) chips were recovered: the partially melted felsite (B) and near-liquidus magma (D), although some chips of D contain micro-xenoliths of B (Figure 4).

Although the actual spatial relationships are unknown, it may be presumed that the high-temperature magma lies below the partially melting felsite. When the magma was penetrated, it rose 8 m from 2104 m to 2096 m within 9 min and then another meter where the bit subsequently became stuck. Lithology C is partially crystallized magma or mush, expected to occur between the melting felsite and the near-liquidus magma (Figure 5), but it is not represented in the chips recovered. 1 mm × 1 mm elemental electron microprobe maps of B and D are shown to the left of the borehole. SiO₂ contents are displayed as false colors indexed on the vertical bar. In B, interstitial rhyolite melt (red ~75 wt% SiO₂) lies between embayed andesine feldspar (lime green, ~56–58 wt% SiO₂) and quartz (white 100 wt% SiO₂). Black denotes cracks and voids. In D, the main component is rhyolite melt (red ~75 wt% SiO₂), with suspended euhedral crystals of andesine (lime green, ~56 wt% SiO₂) and clinopyroxene (dark green ~50 wt% SiO₂). Small black crystals are titanomagnetite (0 wt% SiO₂).

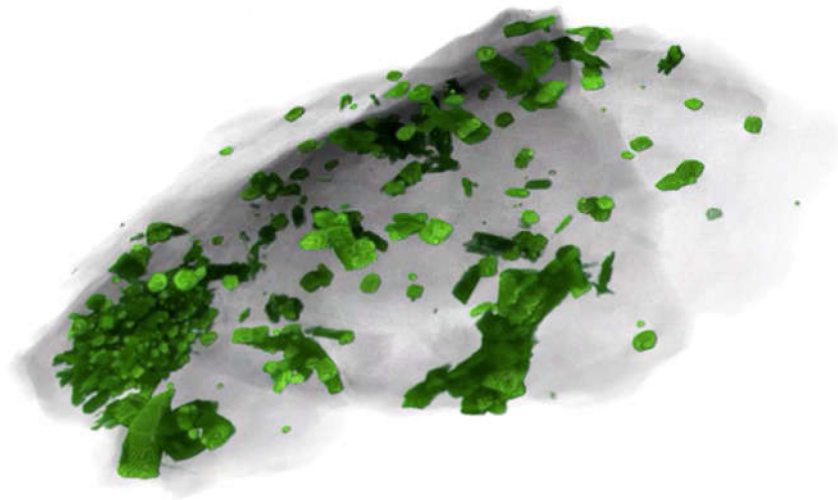


Figure 4. A 3-D perspective by X-ray tomography of a magma chip (2 mm long), from IDDP-1. False-color green crystals, mostly plagioclase, float in transparent gray melt. A clot of crystals at the lower left is partially melted felsite. The chip was quenched at about 2100 m depth and 900 °C. Credit: Sample provided by Landsvirkjun and A. Mortensen; image by F. Wadsworth, Munich U., Germany; E. Saubin, U. of Canterbury and C. I. Schipper, Victoria U., NZ.

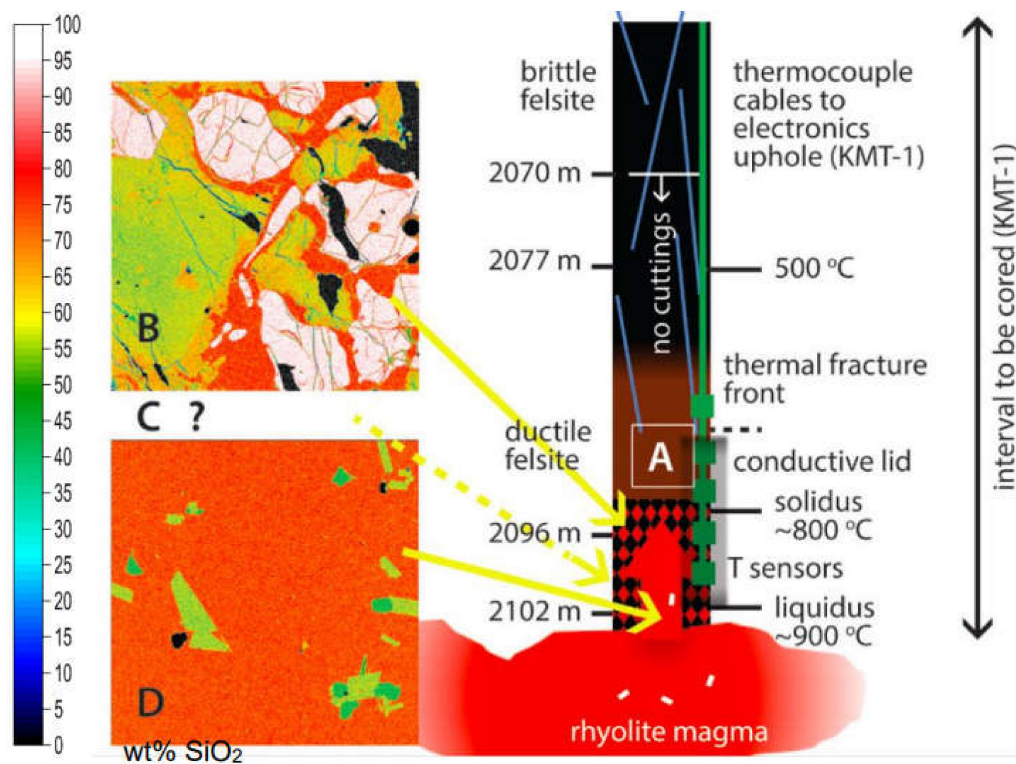


Figure 5. Important observations from the IDDP-1 borehole and 1 mm × 1mm Si element maps of the two lithologies represented in chips from the bottom of the well, color coded in wt% SiO₂ (bar at left). **B** is partially melted felsite, **C** is expected but missing mush, i.e., partially crystallized magma, and **D** is near-liquidus rhyolite magma. Although a layered sequence is shown, it is possible that lithology **B** occurs only as xenoliths (Figure 4) within the magma (**D**). Photo credit: N. Graham and P. Izbekov at University of Alaska Fairbanks’s Advanced Instrumentation Laboratory. Also shown are plans for KMT-1 to obtain continuous core (black double-headed arrow) and a temperature profile from a thermocouple string (green line) through the same interval.

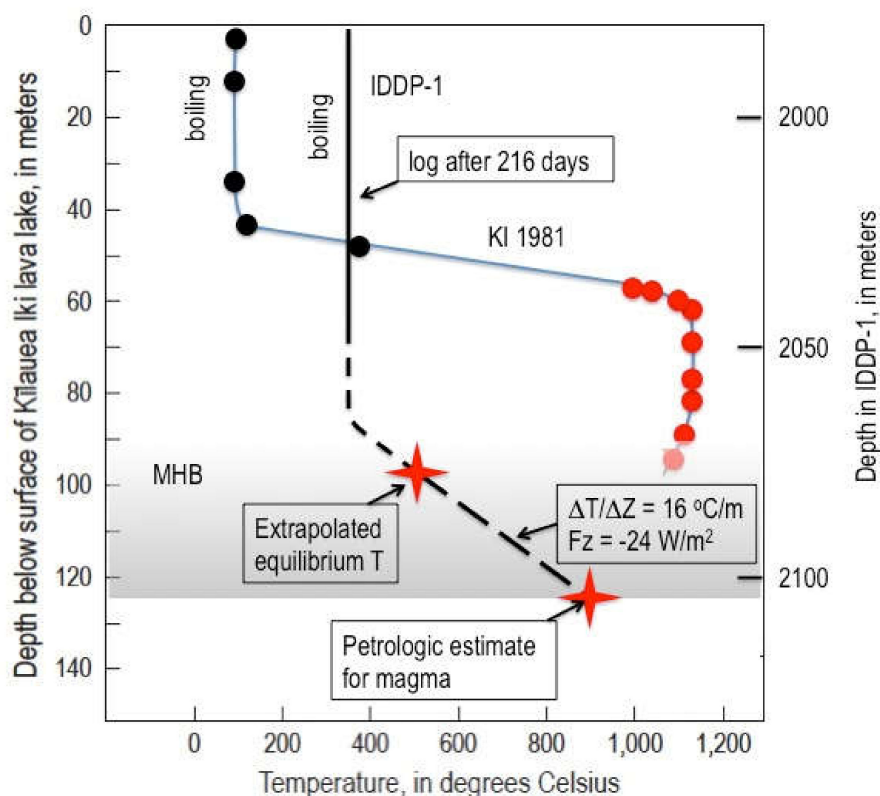


Figure 6. Temperature profile for IDDP-1 [26] compared with Kilauea Iki 1981 [16]. The depth and temperature scales are the same except that a much deeper interval is shown for IDDP-1; hence, the boiling-controlled portion of the profile is hotter. The molten portion in IDDP-1 is rhyolite rather than basalt, so that temperature is lower.

4.1. MHB in Krafla Compared to Kilauea Iki

IDDP-1 provides enough data to place some constraints on the Krafla magma–hydrothermal system. Allowing for the fact that the Krafla results are much deeper than for Kilauea Iki and therefore the hydrothermal temperatures much higher, there is a broad similarity in the temperature profiles. Again, we see an upper hydrothermal zone at the boiling point for the prevailing fluid pressure (Figure 6). Beneath that is a conductive zone with a steep thermal gradient, the MHB. The gradient is constrained by only two temperatures: (1) the time-extrapolated temperature to thermal equilibrium at 2077 m [26] and (2) petrologic estimates for the near-liquidus rhyolite magma, which can be regarded as about 900 ± 50 °C [27,34,35]. This yields a thermal gradient of 16 °C/m.

One of the great mysteries about the rhyolite magma is that it there: shallow yet undetected prior to drilling. Another is that there is no mush zone represented in the cuttings. There is, however, partially melted roof rock, formation of which would seem to require heat from partial crystallization of magma. Krafla is a dominantly basaltic central shield volcano with a summit caldera and essentially no rhyolite eruptions in the last 10^4 a. The very low crystal content would suggest the magma is “new”, yet since the time of the Krafla Fires of 1975 to 1984, the volcano has been among the best monitored in the world [1]. It is unlikely that a substantial body of magma could have arrived at only 2.1 km beneath the center of the volcano during that time period without detection. However, if it were small enough to avoid detection, it should be entirely crystallized.

The existence of a conductive MHB with temperature constraints allows an approach at Krafla analogous to Kilauea Iki to predict how fast crystallization should be occurring in the magma below.

Using Equation (3) and values adopted by Axelsson [28]:

where $\beta_M = 800$ J/kg·°C, sensible heat capacity of rhyolite magma

$L_M = 400,000$ J/kg, latent heat of crystallization of rhyolite magma

$T_L = 900$ °C, liquidus temperature and

$T_S = 800$ °C, solidus temperature [36]

$\rho_M = 2300$ kg/m³, mass density of rhyolite magma

$\rho_R = 2700$ kg/m³, mass density of crystallized rhyolite (felsite)

yields:

$$\beta_{Meff} = 4,800 \text{ J/kg}^\circ\text{C}$$

Equation (4) yields (adjusted to the volume of crystallized rhyolite):

$$\varepsilon_M = 1.3 \times 10^9 \text{ J/m}^3$$

We are neglecting here a contribution from the transfer of energy in any released magmatic vapor phase (MVP [7]), but the amount of vapor exsolved and the pressure and temperature drop it undergoes should be negligible at this local scale.

Applying this to Equation (5) gives:

$$\Delta Z_{800} / \Delta t = 1.9 \times 10^{-8} \text{ m/s or } 0.6 \text{ m/a}$$

This amount of crystallization expected at the roof of the rhyolite magma body over a period of three decades, before which emplacement of the magma might have gone unnoticed, would have been seen in chips from IDDP-1. It is hard to imagine randomly bringing up chips of magma and partially melted felsite without a substantial portion of mush, hypothetical lithology C in Figure 5, if C were present. The simplest interpretation, and one that can be tested by coring, is a stratigraphy comprised downward of felsite (A), partially melted felsite (B), and rhyolite magma (D) with no intervening mush (C). The hotter and higher enthalpy (more melt) rhyolite magma is actively melting its lid (less melt), which in turn means it is releasing heat to the MHB faster than the overlying hydrothermal system can take it away. Presumably, this would be moving MHB upward by effectively dissolving the lower face of MHB and closing fractures by thermal expansion at the cracking front at the upper face. In Kilauea Iki, we clearly see the progress of crystallization yielding mush and then solid crust at the roof of the molten lava lens, and its rate of downward growth is consistent with simple conduction through the MHB. Why not at Krafla? Likely because the magma of Krafla is convecting, and the molten lava of Kilauea Iki is stagnant.

One alternative to the convection of magma under Krafla is that the partially melted felsite is itself the source of the rhyolite magma. Rhyolitic melt could be percolating out of the walls of the bore hole or coming from preexisting segregation veins like those that flowed into the borehole at Kilauea Iki [14]. In this scenario, which aligns with quite a bit of thought about the source of near-liquidus rhyolite [37], the volume below MHB is mostly crystals with interstitial rhyolite melt. However, percolation is a slow process, all the more so with the walls of the borehole quenched. Segregation of melt into veins prior to sampling by drilling seems to be required [38]. However, the magma contains sparse euhedral phenocrysts, totally unlike what is present in the melting felsite. Percolating these through the crystal network of felsite is a physical impossibility. The phenocrysts are larger than the pathways. However, growing them after segregation into veins is equally implausible. The magma and felsite are not in thermal equilibrium. Crystals in the felsite are melting and those in the magma are growing. Heat is being transferred. This could not be so in the segregation vein scenario where veins and their partially melting host should be at the same temperature. There must be flow within the magma relative to the felsite to maintain thermal disequilibrium.

It is worth noting that the calculated minimum heat flux of 24 W/m² in IDDP-1, if applied to the entire area of 3.5 km² that A. Mortensen (2012, unpublished data) suggested, which might be underlain by shallow rhyolitic magma, amounts to only 100 MW thermal power output, or less than the output of IDDP-1 during flow tests and less than the Krafla power plant uses to generate 60 MW electrical power. There are many uncertainties; for example, there may be other magmatic sources of

heat in the caldera, the thermal gradient in MHB could be much higher, or there may be advective transport of heat by magmatic vapor phase through episodic rupturing of MHB [7,9] in addition to continuous conductive transport of heat across MHB. However, if the inferred values approximate reality, then realizing an order of continuous magnitude power output from this magma-sourced geothermal field likely requires penetrating and thermally fracturing MHB, as apparently occurred with IDDP-1.

4.2. MHB Represents a Discontinuity in the Stress Field as Well as in Temperature

Below the MHB is magma with properties of a liquid. As the interval between magma and thermal cracking, MHB is expected to be ductile and should not support a difference between the lithostatic load on it and pressure within the magma. Pressure within the magma can therefore be expected to be lithostatic and isotropic. Above MHB, stress in the rock is lithostatic and anisotropic, whereas fluid in cracks and connected pores is hydrostatic. Hydrostatic pressure in a borehole is a straightforward measurement or calculation. Neglecting additives to water in the drilling fluid (which for some boreholes are substantial) and density variations with temperature, the hydrostatic pressure (P_H) at the bottom of IDDP-1, 2100 m, with fluid standing 400 m below the surface and the density of water $\rho_w = 1,000 \text{ kg/m}^3$, acceleration of gravity $g \sim 10 \text{ m/s}^2$, and depth of water column $z = 1700 \text{ m}$ is:

$$P_H = \rho_w g z \quad (6)$$

$$P_H = 17 \text{ MPa}$$

Taking 2500 kg/m^3 as a common approximation for shallow, porous, and fractured volcanic rock, the lithostatic pressure, P_L , at $z = 2100 \text{ m}$ is:

$$P_L = 53 \text{ MPa}$$

Zierenberg et al. [27] concluded that the magma is at about 40 MPa, less than the lithostatic pressure of 53 MPa, though significantly higher than hydrostatic pressure at 17 MPa, because the volatile content of the quenched melt falls below (i.e., at lower volatile content than) the vapor saturation surface in $\text{CO}_2 + \text{H}_2\text{O}$ vs. P space. Taking this at face value, there are three ways to explain the discrepancy in inferred pressures (1) The rock envelope containing the magma is strong enough to protect it from the full weight of the overburden. This has already been suggested to be unlikely. (2) The magma is vapor undersaturated: i.e., $P_{\text{CO}_2} + P_{\text{H}_2\text{O}} < P_L$. This seems unlikely as well, because the magma appears to have been generated at greater depth by partial melting of hydrothermally altered basalt protolith [27,34,35]. The source rock contained chemically bound water that would be preferentially partitioned into the melt phase. Both partial melting and fractional crystallization concentrate water in melt just as they concentrate other incompatible elements. (3) The magma ascended to a higher level (lower pressure), degassed, and then descended to where it was sampled. This unlikely scenario would be necessary because degassing requires vapor saturation so that volatiles can escape as vapor.

A more likely conclusion is that the magma is vapor saturated at local lithospheric pressure, but the calculated vapor and/or lithostatic pressures are in error. There are multiple possible sources of errors: (1) The actual overburden pressure is unknown. Certainly, the density profile is not constant, and 2500 kg/m^3 is an arbitrary figure. (2) There are uncertainties in the experimentally determined solubility values. (3) Likewise, there are uncertainties in the analytical determination of the CO_2 and H_2O contents, as shown by error bars that overlap the vapor saturation surface at $+1 \sigma$ [27]. (4) Finally, the solubilities of volatiles are dependent on melt temperature, and this is not known with confidence to within $50 \text{ }^\circ\text{C}$. If the magma is hotter than $900 \text{ }^\circ\text{C}$, the solubilities of H_2O and CO_2 will be lower and hence the pressure inferred from the volatile contents higher

There is another intriguing possibility and it arises because of active rifting, the regional stress field is anisotropic with the least principal stress, σ_3 , oriented approximately east–west, causing dikes from

the main basaltic magma system to propagate north–south. Or, if the caldera fill is decoupled from this field, σ_3 may be vertical within the caldera, resulting in the formation of sills. The stress field changes with time during rifting and magma intrusion events. This leads to further uncertainties, not only as to the current confining pressure on the magma but also the history of that pressure. It is possible that the magma degasses if it experiences a lower σ_3 during a rifting event and so becomes vapor undersaturated when pressure returns to equilibrium. The upper limit for pressure in the magma may be σ_3 plus the critical overpressure to initiate a magmatic hydraulic fracture or dike, thought to be < 10 MPa [39]. Therefore, we do not know the pressure on the magma accurately. With the progress presently underway in developing extreme sensors, direct measurement of magma pressure may become possible. This will provide a vast advance in understanding both the coupling of magma dynamics to tectonic events and changes in magma pressure that drive seismicity, surface deformation, and presage eruptions.

In any case, the magma is at or close to vapor saturation and at a much higher pressure than hydrostatic, as dramatically demonstrated by the magma flowing 8 m up IDDP-1 in 9 minutes or less after it was penetrated by drilling [26]. This provides a first direct measurement of magma pressure, although only a crude minimum. When the drill bit reached the magma, there was a weight loss from the drill string (hook load) of 50,000 kg. The magma pushed back with a force in N of $(50,000 \text{ kg}) \times g$. We can treat the drill bit as a piston, albeit an ill-fitting one (Figure 7). Net upward force (F) on the $\frac{1}{4}$ " diameter drill bit is produced by ΔP acting on the area (A) of the bit face:

$$F = \Delta P A \quad (7)$$

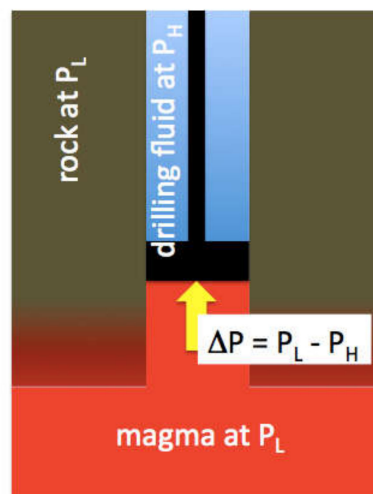


Figure 7. The difference between magma pressure beneath the drill bit and fluid pressure above it supports some of the weight of the drill string.

With a bit area of 0.076 m^2 ($r = 0.15 \text{ m}$):

$$\Delta P = 7 \text{ MPa}$$

We know that $P_H = 17 \text{ MPa}$, so this gives a minimum for P_M of 24 MPa . In fact, magma apparently flowed around and ended up on top of the drill bit at the same time it was pushing against the bit, so clearly the cylinder/piston leaked and $P_M > 24 \text{ MPa}$. This leakage of magma and the fragments of partially melted borehole wall material it carried are the likely sources of the chips that were recovered. The pressure at the top of the rising magma column was also likely reduced by viscous drag as the magma cooled against the borehole walls and drilling fluid.

Note that the large change in the stress field across MHB in Krafla, or between the fluid-filled borehole and its wall, is in contrast to the lava lake case. In the latter, a shallow depth means that the difference between hydrostatic and lithostatic pressure is <2 MPa. The much larger pressure contrast at 2.1 km depth has implications for the stability of the borehole within the MHB at Krafla. Without extensive chilling or emplacement of casing to support ΔP of >30 MPa, the hottest portion of KMT-1 will close much faster than coreholes at Kilauea Iki. This can be used to advantage in understanding the MHB if a thermocouple string can be emplaced quickly (Figure 5) before the borehole closes on it.

4.3. Suppression of Upward Flow of Magma in the Borehole

There is always concern if the fluid in a well is overpressured. However, in general, “overpressured” is relative to hydrostatic. Here, we are dealing with a situation where the fluid, magma, could become overpressured with respect to lithostatic. If the Krafla magma were a simple liquid of $\rho = 2300 \text{ kg/m}^3$, then $P_L = 53 \text{ MPa}$ at 2100 m would support a column of magma 2280 m high, 180 m higher than the surface. However, decompression during ascent would cause exsolution of the CO_2 and H_2O , forming a foam and then a dusty gas (because expansion of magmatic foam is limited by the strength of bubble walls to about 4 X), expanding about 200 X if the pre-eruption magma contains 2 wt% dissolved H_2O , e.g., [40]. This very low-density material within the borehole would reduce the pressure below it, establishing a condition similar to an airlift in a water well, that is, it becomes self-pumping, erupting at high velocity. An eruption, or in drilling terms a blowout, clearly did not happen, and from a safety standpoint in future exploration and use of magma the successful suppression of upward flow needs to be understood. Just as boiling in the drilling fluid column must be prevented, boiling, that is vesiculation, in the magma column, must be prevented as well.

Merely dropping the pressure on the magma to that prevailing at the bottom of the borehole, 17 MPa, results in significant foaming. Neglecting CO_2 , which will not add much to the vapor volume, results from Zierenberg et al. [27] indicate that dropping the pressure of the magma to the hydrostatic pressure of 17 MPa will produce exsolution of about 0.5 wt% H_2O , or 0.005 kg of vapor in 1 kg of magma originally comprising melt (neglecting sparse crystals) with 1.8 wt% dissolved water. For magma density of 2300 kg/m^3 [29], the specific volume is $V_M = 4.3 \times 10^{-4} \text{ m}^3/\text{kg}$. The specific volume of vapor for ideal gas behavior is $V_V = (R \times T)/P$ where $R = 456 \text{ J kg}^{-1} \text{ }^\circ\text{K}^{-1}$, $T = 1173 \text{ }^\circ\text{K}$, and $P = 17 \text{ MPa}$, giving $V_V = 3.1 \times 10^{-2} \text{ m}^3/\text{kg}$ (and consistent with extrapolation from tables of Burnham et al. [41]). The specific volume of the bubble-in-melt suspension is:

$$V_{mix} = X_V^{wt} V_V + X_M^{wt} V_M \quad (8)$$

and porosity, Φ , is:

$$\Phi = V_V / V_{mix} \quad (9)$$

This gives a porosity of 0.27, i.e., 27 vol% bubbles. The magma chips have less porosity than this, and many have no bubble content at all (Figure 4). This is clearly because the chips were effectively quenched by the drilling fluid before vapor exsolution and bubble growth due to decompression could occur. It was the cooling effect of the drilling fluid, rather than the pressure it exerted on the rising magma, that stopped the ascent.

The event described is essentially a small intrusion through an artificial perforation in the MHB. In the same way, a natural breach in MHB will cause quenching of magma unless it has sufficient volume and force to get through the formidable heat sink provided by the hydrothermal system and erupt.

4.4. Convection in Krafla Magma

To explain the absence of crystallization at the top of Krafla magma, Axelsson et al. [29] suggested, and I agree, that there must be convection within the magma body, continually sweeping away denser crystallizing magma and replacing it with uncooled magma at the roof zone (Figure 8).

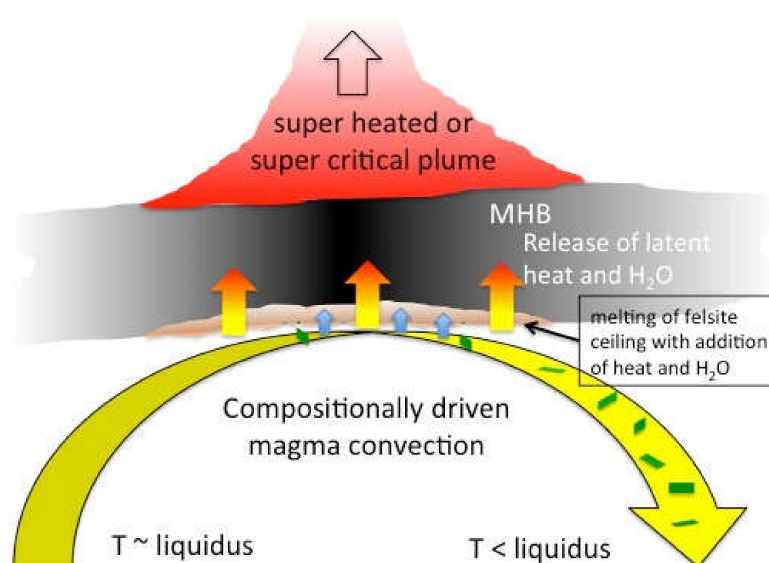


Figure 8. Thermally (density increase due to cooling) and compositionally (density increase due to crystal growth) driven circulation in magma could transfer heat and H₂O at the lower face of the MHB without coating it with crystals and, in the case of Krafla, partially melting it. This would explain the sparse crystal content of all shallow silicic magmas thus far encountered (Table 1).

An independent line of evidence supporting convection is the crystallization required to produce the observed melting in the roof at Krafla. In a static system, crystallization of magma should approximately balance melting in the roof because the latent heat of crystallization dominates the energy budget. Yet the meager crystallization observed at the top of the magma (~1 vol%) cannot account for the much more significant melting observed in some of the felsite (Figure 5). Convection of magma below the static roof would allow the crystallization that is driving the melting to be spread out over a much larger volume of magma, and so crystals would be less abundant in any volume element of magma than melt in a volume element of the roof.

But, melting of the roof requires delivery not only of heat but of water as well. The felsite contains no hydrous phases; it is anhydrous. Without water, the felsite solidus should be about 950 °C [36], well above that of the rhyolite magma with 1.8 wt% H₂O. Two mechanisms might accomplish this transfer of water. One is if the magmatic vapor phase exsolves in the upwelling magma because of decreasing pressure or increasing crystallization (second boiling) or both and enters the overlying felsite along grain boundaries. There it becomes a key though minor (in wt% but not mole%) ingredient in the melt phase as melting develops between quartz and feldspar crystals, which provide the other ingredients necessary to form the eutectic melt. Alternatively, this might be accomplished by diffusion of water within the melt phase. Given the presumed impermeability of MHB and the fact that the diffusivity of water in melt is five orders of magnitude smaller than for heat (10^{-11} m²/s vs. 10^{-6} m²/s), it is probably the transfer of water rather than heat to the felsite that is the rate-controlling step for melting. The extent of melting may therefore be quite limited, perhaps even to only occurring in fragments of roof rock that were engulfed by the magma. As a layer, the partially melted felsite would be a thin transient heat sink, blocking some of the upward heat flow as long as melting is occurring.

The convection hypothesis is consistent with the presence of an upper mush zone in Kilauea Iki and absence in magma bodies. Convection in the former may be limited in time and vigor due to the smaller size and to cooling from the bottom as well as the top in a lava lake, whereas in the magma chamber case, convection may be more vigorous and longer long-term [5].

The simplest form of convection occurs due to thermal contraction of magma on cooling and therefore negative buoyancy at the top of the cooling body. The coefficient of thermal expansion, a , is defined as:

$$a = \frac{1}{V} \frac{\Delta V}{\Delta T} \quad (10)$$

where V is specific volume, about $4 \times 10^{-5} \text{ } ^\circ\text{C}^{-1}$ for magma [5]. The Rayleigh number for thermal convection, Ra_T , which indicates whether a fluid body across which a vertical temperature drop exists will convect, is the dimensionless ratio of the time scale for heat transport by conduction (t_{cd}) divided by the time scale for heat transport by convective flow (t_{cv}).

$$Ra_T = t_{cd}/t_{cv} \quad (11)$$

The time scale for conduction (t_{cd}) can be approximated as d^2/K , where d is the thickness of the magma layer and K is thermal diffusivity of magma. The time scale for convection (t_{cv}) is d/u , where u is the terminal velocity of the sinking cooled fluid, dependent in turn on the density change with cooling (a) and magma viscosity (η). This gives:

$$Ra_T = \frac{\rho \alpha \Delta T d^3 g}{K \eta} \quad (12)$$

Application of the viscosity model of [42] for the Krafla melt composition and $T = 900 \text{ } ^\circ\text{C}$ and $P = 50 \text{ MPa}$ gives viscosity $\eta = 3 \times 10^5 \text{ Pa s}$. Taking $\Delta T = 100 \text{ } ^\circ\text{C}$, $d = 100 \text{ m}$, $K = 10^{-6} \text{ m}^2/\text{s}$, and a as above gives:

$$Ra_T = 3 \times 10^8$$

That is well within the convective regime that begins above $Ra \sim 2000$.

The value of Ra_T is critically dependent upon the thickness of the magma layer, d . A 10-m thickness can be ruled out because the entire body would have crystallized since the Krafla Fires. A thickness of 1000 m is plausible for a long-lived rhyolite magma body. The 100-m thickness is chosen as being intermediate and conservative.

Another route to obtaining magma viscosity is the observation that magma quickly rose 8 m up the borehole after drilling penetrated magma on the second sidetrack [26]. After encountering magma, the drill stem was pulled back and then went back in, encountering magma 8 m higher in the well 9 minutes later. The magma continued to rise as the drill string was pulled back again, and 50,000 kg was lost from the hook load (see Section 4.2). The bit became stuck in magma 9.4 m above the previous level.

The Hagen–Poiseuille equation for fluid flow through a pipe gives a first approximation for this situation, although it applies to steady-state flow rather than abrupt entry of magma into the borehole, wherein the pressure gradient will start high but decrease with time and cooling of magma against the borehole wall and drilling fluid will cause the viscosity to rise.

The equation is:

$$\mu = \frac{\Delta P r^2}{8 V L} \quad (13)$$

Using the same values as in Section 4.2 and velocity $V = 0.015 \text{ m/s}$ and $L = 4 \text{ m}$, the midpoint in flow up the borehole to give an intermediate pressure gradient between the beginning and end of flow, gives:

$$\mu = 2 \times 10^6 \text{ Pa s}$$

This value is about an order of magnitude greater than that calculated from the laboratory measurement-based model of Giodano et al. [42] noted above. However, flow was being impeded by cooling of magma against the borehole walls and the drilling fluid, both raising its viscosity and

constricting the radius (r) of flow. Zierenberg et al. [27] obtained quench temperatures averaging 850 °C based on speciation of water in melt. Dingwell et al. [43] found that a temperature decrease from 900 °C to 800 °C increases viscosity by more than an order of magnitude. So the estimate for magma viscosity from borehole flow is reasonable, but likely higher than that of the undisturbed magma.

There is an additional buoyancy force affecting convection due to crystallization of magma flowing below the roof. As is the case with heat capacity where the effect of heat from crystallization can be added to define an effective heat capacity, the effect of crystallization of crystals denser than melt can be added to obtain an effective thermal expansivity. Just as crystallization dominates heat transport through the release of latent heat, crystallization also dominates mass flow by increasing the bulk density of the melt + crystal mixture, magma.

We should first establish the validity of considering the bulk density of the melt+crystals suspension that is magma, wherein relative motion between melt and crystals can be neglected. The Stokes settling relationship, where buoyancy and drag forces are balanced for a sphere of r radius, is:

$$u = \frac{2 \Delta \rho g r^2}{9 \eta} \quad (14)$$

with $r = 1 \times 10^{-4}$ m (Figure 5), $\Delta \rho = 400$ kg/m³ [29], and $\eta = 3 \times 10^5$ Pa·s [43].

$$u = 3 \times 10^{-11} \text{ m/s}$$

This works out to 1 mm/a, trivial even for convection in a lava lake [5].

The crystallization equivalent for the coefficient of normal thermal expansion, Equation (10), where we will assume linear crystallization with decreasing temperature (not accurate [36] but a useful approximation) from a weight fraction of $X_C^{wt} = 0$ at the liquidus of 900 °C to $X_C^{wt} = 1$ (so that $X_L^{wt} + X_C^{wt} = 1$) at the solidus of 800 °C, is:

$$a_{mix} = \frac{1}{V_{mix}} \frac{\Delta V_{mix}}{\Delta T} \quad (15)$$

where V_{mix} is the specific bulk density of the melt + crystal mixture, i.e., magma:

$$V_{mix} = (X_L^{wt} \times V_L) + (X_C^{wt} \times V_C) \quad (16)$$

Because $X_L^{wt} + X_C^{wt} = 1$, we can deal only with X_C^{wt} as crystallinity, eliminating X_L^{wt} as $(1 - X_C^{wt})$:

$$V_{mix} = V_L + X_C^{wt} \times (V_C - V_L)$$

Because of the relatively small temperature interval, we can treat V_C and V_L as constant with T . Differentiating with respect to T :

$$dV_{mix}/dT = (dX_C^{wt}/dT) \times (V_C - V_L) \quad (17)$$

Using $V_L = 4.35 \times 10^{-4}$ m³/kg, $V_C = 3.70 \times 10^{-4}$ m³/kg, and $dX_C^{wt}/dT = 1/100$ we get:

$$dV_{mix}/dT = 0.65 \times 10^{-6} \text{ m}^3/\text{kg}/^\circ\text{C}$$

Converting to the form of Equation (15) and using a 90:10 liquid to crystal mixture for V_{mix} :

$$a_{mix} = 1.5 \times 10^{-3} \text{ }^\circ\text{C}^{-1}$$

This is almost two orders of magnitude larger than the thermal expansivity of melt, so it will obviously dominate convection if crystallization is occurring, as it must. The compositional Rayleigh number, as it is called, analogous to Equation (12), is then:

$$Ra_C = 4 \times 10^{10}$$

This means that convection will occur in a thinner magma body or at a lower thermal gradient than in the melt-only case.

During convection, there is another process that helps to ensure that the hottest magma is delivered to the base of MHB. That is, the preferential migration of lower viscosity fluid within a fluid of variable viscosity to regions of high shear during flow. This has been observed in the chemical zonation of a volcanic conduit [44] and in pipes in an industrial setting [45]. In convecting magma, the highest shear will be at the base of MHB [45], driving—in addition to the buoyancy forces at work—the hottest magma with least crystallinity there.

However, some caveats should be recognized. One is that crystal growth must be sufficiently rapid to release the latent heat of fusion as the magma is flowing under the roof. If there is a time lag so that crystallization occurs when the magma has already been returned by thermally driven convection to deep in the magma chamber, then it will not contribute to convection as a whole. In fact, it may retard it. Also, in a vapor-saturated system, crystallization of anhydrous phases, as all the crystalline phases in Krafla magma are, will induce vapor exsolution, that is, bubble growth with the vapor fraction dependent upon depth (pressure). This would tend to compensate for the negative buoyancy effect of growing crystals. These complications have been treated in a number of sophisticated models, e.g., [46] and are beyond the scope of this simple analysis. The conclusion here is that the release of latent heat and forcing convection by crystallization are linked and can contribute greatly to heat transport from magma into the suprajacent hydrothermal system. Arguments against convection of magma, both experimental and theoretical, rely on growth crystals at the roof of the magma body in response to heat lost through MHB. Thus far, drilling encounters with magma indicate that this is not the case. A difference in views is whether convection is limited to the earliest stage of a magma body and therefore can be ignored in its overall cooling history [47] or whether it can continue until flow is locked as the crystal content approaches 50 vol% [4].

To get an idea of how effective convection is in delivering heat to MHB, we can ask how large the upwelling limb of magma convection cell needs to be to continuously deliver 1 GW of thermal energy. Assumptions are a vertical velocity in cross sectional area A , rising at vertical velocity u , say 0.01 m/s, and releasing heat to the roof by cooling 10 °C.

$$P_T = X_C^{wr} \beta_{Meff} A u \quad (18)$$

Using the same parameters as before and solving for the radius of the heat pipe:

$$r = 17 \text{ m}$$

There may be time-discontinuous mechanisms of heat transport as well, for example, magma breaching the MHB and cooling within the hydrothermal system, transferring its energy directly. Based upon observations at Yellowstone, including inflation and deflation cycles and migrating seismic swarms, Fournier [9] postulated that build up of vapor pressure in a magma body due to crystallization would periodically rupture the MHB, injecting the magmatic vapor phase into the hydrothermal system (and occasionally causing phreatomagmatic eruptions).

4.5. Conceptual Model of Krafla as a Closely Coupled Magma–Hydrothermal System

A view of the Krafla system that is consistent with, but not unique to, most of the observations cited is presented in Figure 9. Like its nearby companion, Askja Caldera [33], Krafla is an essentially

basaltic system lying astride Iceland's northern rift zone. Although one might be tempted to think of rift magmatism as uniformly distributed along the spreading plate boundary, these central volcanoes are clearly foci of basaltic magma upwelling that then feed dikes laterally at shallow depth along the rift structure. If there is a deeper zone of uniform along-strike magma generation, the magma must gather into plumes or heat pipes, which in this case then feeds into chambers or dike/sill complexes that in turn redistribute magma laterally at shallower depth. In a way, this is like subduction zone volcanism where existing models suggest uniform, along-strike magma generation above the subducting slab that coalesces upward to focus into discrete, long-lived centers rooted in the crust.

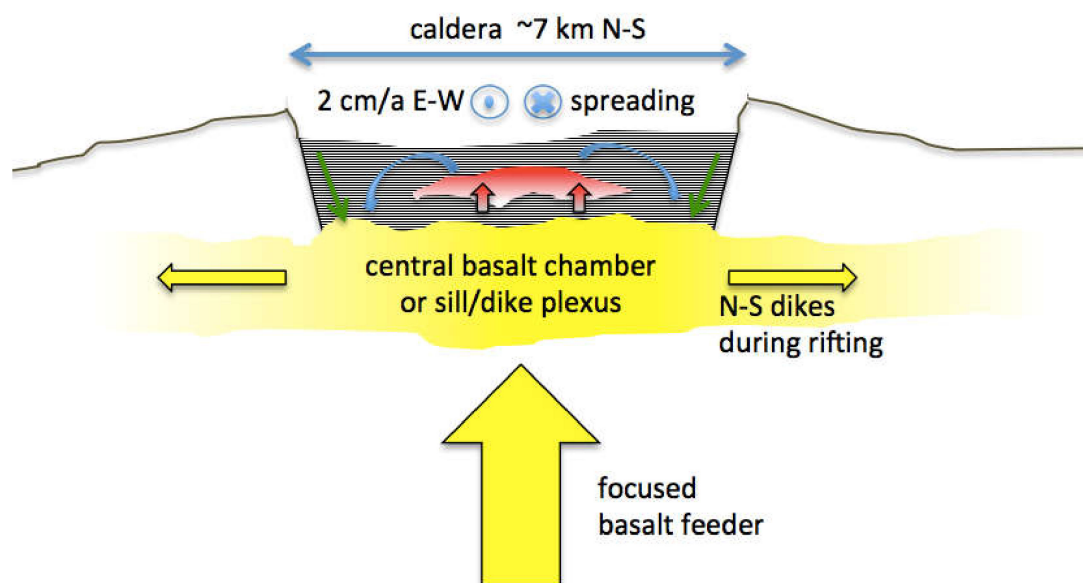


Figure 9. Suggested concept for Krafla shield and caldera. A basaltic magma plume beneath the rift is responsible for building the shield and maintaining a large and relatively shallow basaltic magma chamber. This chamber may be a plexus of dykes and sills rather than an oblate bladder. During rifting events, the magma accumulation feeds dikes that travel tens of kilometers to the north and south, deflating and contributing to caldera subsidence in the process. Central eruptions and intrusions of basalt and more silicic magmas comprise the caldera fill, which is hydrothermally altered in this crucible and gradually fed downward to the basaltic hearth. Partial melting ensues, probably continuously dribbling rhyolitic melt upward to its level of neutral buoyancy at about 2 km depth. If the input is insufficient, only felsite sills are produced, but if more vigorous, a homogeneous convecting rhyolite magma body is established. It is stable for long periods of time, but can be expelled if a massive influx of basaltic magma occurs below it during a major rifting event. Undisturbed, the shallow rhyolite contributes only a portion of the thermal output of the caldera, but it represents a massive concentration of latent heat of crystallization at shallow depth that can be accessed if the MHB above it is penetrated by drilling, allowing fluid to invade and fracture the magma and near-magma region.

Sustained, focused magmatism produces impressive edifices, but less so in rifts because the structures are being torn apart as they are built. Focused magmatism also produces calderas that are the surface expression of shallow magma chambers. As such, calderas reflect subsidence above shallow magma bodies because over time the magma entering the chamber is more than balanced by magma dispersed beyond the immediate volcanic center. The two processes that do this are lateral diking that drains the central chamber in the subsurface and large volume explosive eruptions that disperse its contents widely on the surface. The former is more frequent and the latter more catastrophic. Both processes appear to have contributed to the topographically rather subtle Krafla Caldera.

The association of rhyolitic magmas with an isotopic signature suggestive of a hydrothermally altered basalt protolith [27] fits with this view. Intense hydrothermal circulation is concentrated within

these caldera structures, and the gradual or episodic subsidence feeds hydrothermally altered basaltic caldera fill towards the hot plate of focused basaltic magmatism. Partial melting ensues, generating rhyolitic melt that accumulates at shallow depth, perhaps at its level of neutral buoyancy, as a coherent body. This may be a continuous process and requires only local vertical rearrangement of materials. Thus it produces little by way of surface deformation or gravity signals. Being viscous and at neutral buoyancy, the magma accumulation remains stable over millennia, requiring a massive “kick” by a basaltic intrusion as occurred at Askja [33] in 1875 or on a smaller scale at Krafla’s Viti Crater in 1724 [20]. To remain near liquidus, these rhyolitic accumulations must themselves be continuously heated by the basaltic furnace, either through their own intervening conductive boundary zone, or directly, because the strong contrast in density and viscosity and relatively low water content inhibit mixing [48]. Indeed, Iceland is one of the classic sites exhibiting bimodal volcanism [49]. This is in contrast to the subduction zone case where high water contents in the basalt cause foaming and mixing due to the temperature contrast at the boundary [50].

This is an admittedly simplistic picture, and three variants in the magma–hydrothermal relationship seem obvious. One is where the shallow magma body maintains an open pathway to the surface. This prevents the hydrothermal system from forming as a cap above the magma, but allows it to develop as a lateral fluid outflow zone. Mutnovsky Volcano, Kamchatka, Russia, is an example [51]. The direct connection between Mutnovsky and its adjacent geothermal system is supported both by oxygen isotope composition of fluids and evidence that changes in geothermal energy extraction appear to modulate the behavior of the volcano itself (A. Kiryukhin, unpublished data, 2019). Another is the rift setting, such as Reykjanes or in submarine midocean ridges, where frequent unfocused dike events maintain high temperature fluid circulation in the crust. The development of a magma chamber requires frequent, focused input [11]. Finally, as the end stage of a silicic system, the melt may disappear and with hydrothermal circulation driven by residual heat. However, in this case, shallow heat is not replenished by the combination of the latent heat of crystallization and magma convection.

5. Magma as an Energy Source for Geothermal Power Production

It is useful to consider energy density as it varies within a magma–hydrothermal system. This reveals where the energy is stored and what volume must be accessed to produce a thermal power output over a given period of time. Ultimately, whether by natural process or enhanced to extract geothermal energy, heat transport is some combination of short path-length conduction and long-path length convection. The enthalpy of hydrothermal fluid is important in that it determines how rapidly energy can be transported within a hydrothermal system and out of it for geothermal power production. However, because the fluid occupies only pores and fractures within a hydrothermal reservoir, it does not contribute much to the total energy in the system.

For magma as the source of energy, we need to consider energy per liquid volume (2300 kg/m³) rather than its crystallized product (2700 kg/m³) calculated previously. This yields:

$$\varepsilon_R = 1.1 \times 10^9 \text{ J/m}^3$$

In this case, I include the enthalpy of the 2 wt% H₂O that will be released as the magma crystallizes and eventually adds to power output at the surface. For water at 50 MPa and 800 °C [41], the enthalpy is 4 × 10⁹ J/kg. Added to the magma, this yields a total energy density of:

$$\varepsilon_R = 1.3 \times 10^9 \text{ J/m}^3$$

There are processes not considered here that reduces the total energy in magma. One is the heat of vesiculation, which is opposite in sign from heat of crystallization. Another is any work, $P\Delta V$, done by expansion of the system against pressure as it exsolves the magmatic vapor phase. However, Sahagian and Proussevich [52] have shown that these energy terms can be neglected.

The Krafla magma is shallow and fairly dry. For magmas with the more typically estimated 4–6 wt%, the additional enthalpy in expelled magmatic vapor is more significant and may play an important role in mass and heat transfer, particularly during the latter half of the crystallization history of a magma body [7].

A useful reference amount of energy, say Q_{30} , is an amount required to produce 1 GW of thermal power output for 1 Gs, or about 30 a, a standard business horizon and also about 10^9 s. The volume of Krafla-like magma required is 0.8 km^3 . For visualization purposes, the face of the monolith El Capitan, Yosemite National Park, California, USA, is roughly 1 km^2 , so a cube extending 800 m into it would be 0.8 km^3 . That is not to say that all the energy would be extractable, especially since convection would cease before 50% crystallization is reached, and heat transport would then be limited to invasion of the hydrothermal system by thermal cracking towards the hot center.

By comparison, for the same temperature drop in solid rock with 5 vol% superheated fluid in pores at 50 MPa and $800 \text{ }^\circ\text{C}$, the contribution of superheated fluid in pores, even at $4 \times 10^6 \text{ J/kg}$, is insignificant (0.2 wt%) and (Figure 10):

$$\varepsilon = 2.2 \times 10^8 \text{ J/m}^3$$

$$V = 4.5 \text{ km}^3$$

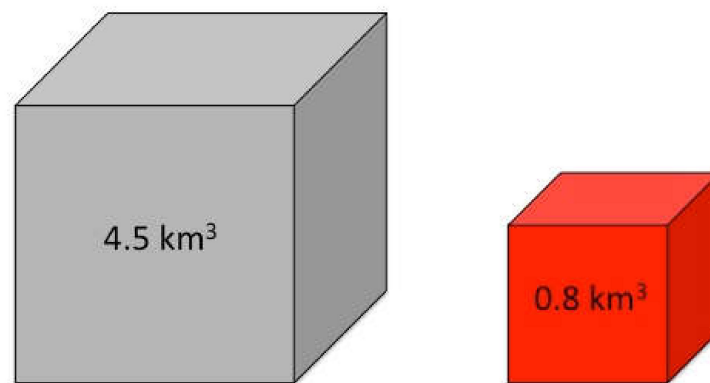


Figure 10. The volume of rock (gray) or magma (red) required to release 10^9 GJ of thermal energy during cooling of $\Delta T = 100 \text{ }^\circ\text{C}$. For the magma, the temperature drop is chosen to be liquidus to solidus, thereby releasing all the latent heat of crystallization. For the rock, where the energy content is entirely sensible heat, only the size of the temperature interval is important.

Accepting the argument that conduction through the MHB is the rate-controlling step for heat transport, then it also controls the response time over which a perturbation in the magma reservoir or hydrothermal reservoir will affect the other part of the system. Such a perturbation might be due to a new influx of very hot magma heating the magma reservoir, as, for example, with the Krafla Fires of 1975–1984 [20], or initiation of geothermal power production, cooling the hydrothermal reservoir as at Mutnovsky [51].

The characteristic time, τ , for thermal diffusion where ΔZ is the thickness of the MHB and K is thermal diffusivity is:

$$\tau = \Delta Z^2 / K \quad (19)$$

Taking 25 m as the upper limit of ΔZ at Krafla and $K = 10^{-6} \text{ m}^2/\text{s}$,

$$\tau = 6.3 \times 10^8 \text{ s or about 20 a}$$

This is on the threshold of geothermal production by humans influencing magmatic behavior. If the actual value is $\Delta Z = 10$ m, then $\tau = 3$ a, which is to say that the power plant is actually tapping magma energy. Because the geothermal energy extraction is increasing cooling at the top of the magma body, the response may be to accelerate convection, thereby pulling thermal energy from deeper in the body. On the other hand, if the magmatic heat source is distant, say 500 m, then $\tau = 10^4$ a and the two reservoirs are effectively separate. Put another way, exploitation of the hydrothermal system would be mining old magmatic heat.

6. Applications

The picture of the Krafla system painted here, if a general case, would imply that magma-related geothermal systems contain far more energy, with higher enthalpy fluids, and are more sustainable than would otherwise be expected. The key may be to penetrate the MHB, by drilling and thermal cracking, so that hydrothermal fluid gains access to the magma itself. Convection within the magma, supplying latent heat of crystallization, enthalpy of magmatic vapor phase from a voluminous source, combined with continued thermal cracking due to energy extraction, could maintain thermal power output without or with lesser need of makeup wells. We need to test this scenario with space-continuous samples and temperature measurements through the MHB at Krafla, and at multiple points in time. We also need to improve geophysical techniques for imaging magma. Such prospecting tools have been tested against reality and improved through much drilling experience in the case of oil and gas reservoirs, but this was never, until now, possible for testing the imaging of magma reservoirs.

There are also large challenges in drilling engineering and technology, because for superhot geothermal power generation, production wells must be sustainable over a long period. This challenge encompasses casing alloys, accommodation of thermally induced stresses in casing, cementing at high pressure and temperature, corrosion and precipitation by and from acid fluids, and extreme sensor technology. The objection that truly high-grade geothermal systems are too far from the customer base to be viable is diminished by recent applications of High Voltage Direct Current (HVDC) technology that enables transmission of electrical power over great distances, including under the ocean, without losses due to the conductor skin effect and external inductive field of AC.

Development of extreme sensor technology, now underway for combustion engine and planetary exploration applications, opens another use for which there is a compelling need: monitoring of restless volcanoes and forecasting of eruptive events [12,53]. All the sensors used to date for volcano monitoring, which measure thermal and gas emission, surface deformation, and seismicity, are in essence remote sensing techniques that are interpreted but not tested against ground truth to reflect processes in the source magma that may or may not lead to eruption. Direct measurement of conditions within or at least proximal to magma bodies would test and improve these interpretations and in the case of very high risk volcanoes might partially supplant labor-intensive surface-based multisensor networks themselves. Monitoring temperature in magma is already within our grasp. Inflation, increased CO₂ and thermal emission, and increased seismicity are often interpreted as the rise of new magma into a shallow magma chamber, portending an eruption. This should quickly cause a temperature rise in the convecting magma body being intruded and therefore detected and quantified by in situ sensors. Another, and perhaps simpler question that could be answered, and always arises during periods of volcano unrest, is: are the geophysical and geochemical signals a consequence of underlying magmatic processes or merely reflecting of some structural reconfiguration within the hydrothermal system?

Accidental drilling encounters with magma are beginning to provide new insights into the relationship between magma and hydrothermal systems. Encounters planned for scientific and engineering objectives, as, for example, proposed for the Krafla Magma Testbed (KMT) [12,54], have the potential to lead to a new, much needed clean bedload electric energy source and a reliable means to warn populations at risk of impending eruptions. The scientific, geothermal energy, and

volcanic hazard needs are compelling. It seems likely therefore that planned explorations of this new frontier are both essential and inevitable.

7. Conclusions

Existing in situ data from magma bodies are few and without precedent. Data from Krafla confirm the existence of an MHB such as found in lava lake drilling and predicted from theoretical considerations. The MHB at Krafla is remarkably thin. However, with such sparse data, it is not possible to say how representative Krafla is of magma–hydrothermal systems in general. Combining Krafla results with insights from the two other sites of magma encounters and results from lava lake drilling, it is suggested that:

- The MHB is a moving boundary. It can ascend by melting of the magma ceiling if the magma heats up or descend by thermal cracking, ultimately to the center of the magma body as it cools.
- The MHB is not only a thermal boundary but also a stress field boundary because of the upward transition from fluid to ductile to brittle behavior. It forms a barrier between magma where pressure is isotropic and lithostatic, and above which stresses are anisotropic and lithostatic within rock, and isotropic and hydrostatic in fluid-field fractures. Understanding this is essential to understanding the processes of volcano unrest and eruption.
- Although heat transport through the MHB is impressive, it is of the same order as conventional geothermal power extraction. The order of magnitude increase in thermal power output of near-magma wells likely requires penetrating and thermally cracking the MHB. Once done, crystallization-driven convection within the magma body, release of the magmatic vapor phase, and continued thermal fracturing by induced fluid circulation may make much of the energy contained within magma accessible for use.
- First-order data needed to understand magma–hydrothermal coupling are continuous petrological (core) and temperature profiles across the MHB, from solid, brittle rock to near-liquidus magma. In view of the apparent difficulty of magma breaching the MHB, using pressure sensors to detect an increase in magma pressure may be an effective way to predict eruptions. These advances, ultimately leading to exploitation of magma energy and reliable eruption forecasting, will require a testbed approach of multiple boreholes and engineering and scientific experiments over an extended period of time.

Funding: I benefited from workshops on the Krafla Magma Testbed supported by Landsvirkjun National Power Company, International Continental Scientific Drilling Program (ICDP), and the US National Science Foundation (NSF). In addition, I received travel support from Landsvirkjun, Iceland; the Geothermal Research Group (GEORG), Iceland; and the British Geological Survey.

Acknowledgments: Thanks are due for discussions with many colleagues involved in the Krafla Magma Testbed Project and for the pioneering work of IDDP. I am especially grateful to Charles Carrigan, Yan Lavallee, Allen Glazner, and Pavel Izbekov for stimulating insights, many of which are cited here, but that is not to say that they agree with everything herein. Charles Carrigan and Pavel Izbekov contributed to magma viscosity calculations.

Conflicts of Interest: I declare that I have no competing financial interests or personal relationships that could have influenced the work reported in this paper.

References

1. Lister, C.R.B. On the Penetration of Water into Hot Rock. *Geophys. J. Int.* **1974**, *39*, 465–509. [[CrossRef](#)]
2. Hardee, H.C. Solidification in Kilauea Iki lava lake. *J. Volcanol. Geotherm. Res.* **1980**, *7*, 211–223. [[CrossRef](#)]
3. Carrigan, C.R. Biot number and thermos bottle effect: Implications for magma-chamber convection. *Geology* **1988**, *16*, 771–774. [[CrossRef](#)]
4. Carrigan, C.R. Time and temperature dependent convection models of cooling reservoirs: Application to volcanic sills. *Geophys. Res. Lett.* **1984**, *11*, 693–696. [[CrossRef](#)]
5. Carrigan, C.R. The magmatic Rayleigh number and time dependent convection in cooling lava lakes. *Geophys. Res. Lett.* **1987**, *14*, 915–918. [[CrossRef](#)]

6. Hort, M.; Marsh, B.D.; Resmini, R.G.; Smith, M.K. Convection and Crystallization in a Liquid Cooled from above: An Experimental and Theoretical Study. *J. Petrol.* **1999**, *40*, 1271–1300. [[CrossRef](#)]
7. Lamy-Chappuis, B.; Heinrich, C.A.; Driesner, T.; Weis, B. Mechanisms and patterns of magmatic fluid transport in cooling hydrous intrusions. *Earth Planet. Sci. Lett.* **2020**, *535*, 116111. [[CrossRef](#)]
8. Hawkesworth, C.J.; Blake, S.; Evans, P.; Hughes, R.; Macdonald, R.; Thomas, L.E.; Turner, S.P.; Zellmer, G. Time Scales of Crystal Fractionation in Magma Chambers—Integrating Physical, Isotopic and Geochemical Perspectives. *J. Petrol.* **2000**, *41*, 991–1006. [[CrossRef](#)]
9. Fournier, R.O. Geochemistry and Dynamics of the Yellowstone National Park Hydrothermal System. *Annu. Rev. Earth Planet. Sci.* **1989**, *17*, 13–53. [[CrossRef](#)]
10. Scott, S.; Driesner, T.; Weis, P. Boiling and condensation of saline geothermal fluids above magmatic intrusions. *Geophys. Res. Lett.* **2017**, *44*, 1696–1705. [[CrossRef](#)]
11. Glazner, A.F. Climate and the Development of Magma Chambers. *Geosciences* **2020**, *10*, 93. [[CrossRef](#)]
12. Eichelberger, J. Magma: A journey to inner space. *EOS* **2019**, *100*, 26–31.
13. Cashman, K.V.; Sparks, R.S.J.; Blundy, J.D. Vertically extensive and unstable magmatic systems: A unified view of igneous processes. *Science* **2017**, *355*, eaag3055. [[CrossRef](#)] [[PubMed](#)]
14. Colp, J.L. “Final Report-Magma Energy Research Project”; Sand82-2377; Sandia National Laboratories: Albuquerque, NM, USA, 1982; pp. 1–36.
15. Barth, G.A.; Kleinrock, M.C.; Helz, R.T. The magma body at Kilauea Iki lava lake: Potential insights into mid-ocean ridge magma chambers. *J. Geophys. Res.* **1994**, *99*, 7199–7217. [[CrossRef](#)]
16. Helz, R.T.; Clague, D.A.; Sisson, T.W.; Thornber, C.R. Petrologic insights into basaltic volcanism at historically active Hawaiian volcanoes. *Prof. Pap.* **2014**, 237–292. Available online: https://www.researchgate.net/profile/Rosalind_Helz/publication/271829142_Petrologic_Insights_into_Basaltic_Volcanism_at_Historically_Active_Hawaiian_Volcanoes/links/54d2698b0cf25017917dfedc.pdf (accessed on 26 May 2020).
17. Teplow, W.; Marsh, B.; Hulen, J.; Spielman, P.; Kaleikini, M.; Fitch, D.; Rickard, W. Dacite melt at the Puna geothermal venture wellfield, Big Island of Hawaii. *Geotherm. Resour. Counc. Trans.* **2009**, *33*, 989–994.
18. Mbia, P.K.; Mortensen, A.K.; Oskarsson, N.; Hardarson, B. Sub-surface geology, petrology and hydrothermal alteration of the Menengai geothermal field, Kenya: Case study of wells MW-02, MW-04, MW-06 and MW-07. In Proceedings of the World Geothermal Congress, Melbourne, Australia, 19–25 April 2015; p. 20.
19. Mibei, G.; Lagat, J. Structural controls in Menengai geothermal field. In Proceedings of the Kenyatta International Conference Centre, Nairobi, Kenya, 21–22 November 2011; p. 21.
20. Árnason, K. New Conceptual Model for the Magma–hydrothermal–Tectonic System of Krafla, NE Iceland. *Geosci. J.* **2020**, *10*, 34. [[CrossRef](#)]
21. Elders, W.A.; Friðleifsson, G.Ó.; Albertsson, A. Drilling into magma and the implications of the Iceland Deep Drilling Project (IDDP) for high-temperature geothermal systems worldwide. *Geothermics* **2014**, *49*, 111–118. [[CrossRef](#)]
22. Glazner, A.F.; Bartley, J.M.; Coleman, D.S. We need a new definition for “magma”. *EOS* **2016**, *97*, 12–13. [[CrossRef](#)]
23. Björnsson, H.; Björnsson, S.; Sigurgeirsson, T. Penetration of water into hot rock boundaries of magma at Grímsvötn. *Nature* **1982**, *295*, 580–581. [[CrossRef](#)]
24. Reynolds, H.I.; Gudmundsson, M.T.; Högnadóttir, T.; Pálsson, F. Thermal power of Grímsvötn, Iceland, from 1998 to 2016: Quantifying the effects of volcanic activity and geothermal anomalies. *J. Volcanol. Geotherm. Res.* **2018**, *358*, 184–193. [[CrossRef](#)]
25. Haddadi, B.; Sigmarsson, O.; Devidal, J.-L. Determining intensive parameters through clinopyroxene-liquid equilibrium in Grímsvötn 2011 and Bárðarbunga 2014 basalts. In Proceedings of the Geophysical Research Abstracts, Vienna, Austria, 24–25 April 2015; Volume 17. EGU General Assembly.
26. Mortensen, A.K.; Egilson, P.; Gautason, B.; Árnadóttir, S.; Guðmundsson, Á. Stratigraphy, alteration mineralogy, permeability and temperature conditions of well IDDP-1, Krafla, NE-Iceland. *Geothermics* **2014**, *49*, 31–41. [[CrossRef](#)]
27. Zierenberg, R.A.; Schiffman, P.; Barfod, G.H.; Leshner, C.E.; Marks, N.E.; Lowenstern, J.B.; Mortensen, A.K.; Pope, E.C.; Bird, D.K.; Reed, M.H.; et al. Composition and origin of rhyolite melt intersected by drilling in the Krafla geothermal field, Iceland. *Contrib. Mineral. Petrol.* **2013**, *165*, 327–347. [[CrossRef](#)]
28. Carslaw, H.S.; Jaeger, J.C. *Conduction of Heat in Solids*, 2nd ed.; Clarendon Press: Oxford, UK, 1959.

29. Axelsson, G.; Egilson, T.; Gylfadóttir, S.S. Modelling of temperature conditions near the bottom of well IDDP-1 in Krafla, Northeast Iceland. *Geothermics* **2014**, *49*, 49–57. [[CrossRef](#)]
30. Lamur, A.; Lavallée, Y.; Iddon, F.E.; Hornby, A.J.; Kendrick, J.E.; von Aulock, F.W.; Wadsworth, F.B. Disclosing the temperature of columnar jointing in lavas. *Nat. Commun.* **2018**, *9*, 1–7. [[CrossRef](#)] [[PubMed](#)]
31. Schuler, J.; Greenfield, T.; White, R.S.; Roecker, S.W.; Brandsdóttir, B.; Stock, J.M.; Tarasewicz, J.; Martens, H.R.; Pugh, D. Seismic imaging of the shallow crust beneath the Krafla central volcano, NE Iceland. *J. Geophys. Res.* **2015**, *120*, 7156–7173. [[CrossRef](#)]
32. Kim, D.; Brown, L.D.; Árnason, K.; Águstsson, K.; Blanck, H. Magma reflection imaging in Krafla, Iceland, using microearthquake sources. *J. Geophys. Res.* **2017**, *122*, 5228–5242. [[CrossRef](#)]
33. Sigurdsson, H.; Sparks, R.S.J. Petrology of Rhyolitic and Mixed Magma Ejecta from the 1875 Eruption of Askja, Iceland. *J. Petrol.* **1981**, *22*, 41–84. [[CrossRef](#)]
34. Schiffman, P.; Zierenberg, R.A.; Mortensen, A.K.; Friðleifsson, G.Ó.; Elders, W.A. High temperature metamorphism in the conductive boundary layer adjacent to a rhyolite intrusion in the Krafla geothermal system, Iceland. *Geothermics* **2014**, *49*, 42–48. [[CrossRef](#)]
35. Masotta, M.; Mollo, S.; Nazzari, M.; Tecchiato, V.; Scarlato, P.; Papale, P.; Bachmann, O. Crystallization and partial melting of rhyolite and felsite rocks at Krafla volcano: A comparative approach based on mineral and glass chemistry of natural and experimental products. *Chem. Geol.* **2018**, *483*, 603–618. [[CrossRef](#)]
36. Hammer, J.E.; Rutherford, M.J. An experimental study of the kinetics of decompression-induced crystallization in silicic melt. *J. Geophys. Res.* **2002**, *107*, ECV-8. [[CrossRef](#)]
37. Bachmann, O.; Bergantz, G.W. On the origin of crystal-poor rhyolites: Extracted from batholithic crystal mushes. *J. Petrol.* **2004**, *45*, 1565–1582. [[CrossRef](#)]
38. Helz, R.T. Crystallization history of Kilauea Iki lava lake as seen in drill core recovered in 1967–1979. *Bull. Volcanol.* **1980**, *43*, 675–701. [[CrossRef](#)]
39. Rubin, A.M. Tensile fracture of rock at high confining pressure: Implications for dike propagation. *J. Geophys. Res.* **1993**, *98*, 15919. [[CrossRef](#)]
40. Eichelberger, J.C.; Carrigan, C.R.; Westrich, H.R.; Price, R.H. Non-explosive silicic volcanism. *Nature* **1986**, *323*, 598–602. [[CrossRef](#)]
41. Burnham, C.W.; Holloway, J.R.; Davis, N.F. Thermodynamic Properties of Water to 1,0000 C and 10,000 Bars. *Geol. Soc. Am.* **1969**, *132*, 96.
42. Giordano, D.; Russell, J.K.; Dingwell, D.B. Viscosity of magmatic liquids: A model. *Earth Planet. Sci. Lett.* **2008**, *271*, 123–134. [[CrossRef](#)]
43. Dingwell, D.B.; Romano, C.; Hess, K.-U. The effect of water on the viscosity of a haplogranitic melt under PTX conditions relevant to silicic volcanism. *Contrib. Mineral. Petrol.* **1996**, *124*, 19–28. [[CrossRef](#)]
44. Carrigan, C.R.; Eichelberger, J.C. Zoning of magmas by viscosity in volcanic conduits. *Nature* **1990**, *343*, 248–251. [[CrossRef](#)]
45. Stockman, H.W.; Cygan, R.T.; Carrigan, C.R. Modelling viscous segregation in immiscible fluids using lattice-gas automata. *Nature* **1990**, *348*, 523–525. [[CrossRef](#)]
46. Cardoso, S.S.S.; Woods, A.W. On convection in a volatile-saturated magma. *Earth Planet. Sci. Lett.* **1999**, *168*, 301–310. [[CrossRef](#)]
47. Brandeis, G.; Marsh, B.D. The convective liquidus in a solidifying magma chamber: A fluid dynamic investigation. *Nature* **1989**, *339*, 613–616. [[CrossRef](#)]
48. Eichelberger, J.C.; Gooley, R. Evolution of silicic magma chambers and their relationship to basaltic volcanism. In *The Earth's Crust*; IntechOpen: London, UK, 1977; pp. 57–77.
49. Eichelberger, J.C. Andesitic volcanism and crustal evolution. *Nature* **1978**, *275*, 21–27. [[CrossRef](#)]
50. Eichelberger, J.C. Vesiculation of mafic magma during replenishment of silicic magma reservoirs. *Nature* **1980**, *288*, 446–450. [[CrossRef](#)]
51. Kiryukhin, A.; Chernykh, E.; Polyakov, A.; Solomatina, A. Magma Fracking Beneath Active Volcanoes Based on Seismic Data and Hydrothermal Activity Observations. *Geosci. J.* **2020**, *10*, 52. [[CrossRef](#)]
52. Sahagian, D.L.; Proussevitch, A.A. Thermal effects of magma degassing. *J. Volcanol. Geotherm. Res.* **1996**, *74*, 19–38. [[CrossRef](#)]

53. Lowenstern, J.B.; Sisson, T.W.; Hurwitz, S. Probing magma reservoirs to improve volcano forecasts. *EOS* **2017**, *98*. Available online: https://www.researchgate.net/profile/Jacob_Lowenstern/publication/320588486_Probing_Magma_Reservoirs_to_Improve_Volcano_Forecasts/links/59f937f3aca272607e2f71a4/Probing-Magma-Reservoirs-to-Improve-Volcano-Forecasts.pdf (accessed on 26 May 2020). [CrossRef]
54. Eichelberger, J.C.; Carrigan, C.R.; Ingolfsson, H.P.; Lavallee, Y.; Ludden, J.; Markussón, S.; Mortensen, A.; Papale, P.; Sigmundsson, F.; Saubin, E.; et al. Magma-sourced geothermal energy and plans for krafla magma testbed, iceland. In Proceedings of the World Geothermal Congress, Reykjavik, Iceland, 27 April–1 May 2020.



© 2020 by the author. Licensee MDPI, Basel, Switzerland. This article is an open access article distributed under the terms and conditions of the Creative Commons Attribution (CC BY) license (<http://creativecommons.org/licenses/by/4.0/>).